

## Regime shifts occur disproportionately faster in larger ecosystems

Cooper, Gregory; Willcock, Simon; Dearing, John

### Nature Communications

DOI:  
[10.1038/s41467-020-15029-x](https://doi.org/10.1038/s41467-020-15029-x)

Published: 10/03/2020

Peer reviewed version

[Cyswllt i'r cyhoeddiad / Link to publication](#)

*Dyfyniad o'r fersiwn a gyhoeddwyd / Citation for published version (APA):*  
Cooper, G., Willcock, S., & Dearing, J. (2020). Regime shifts occur disproportionately faster in larger ecosystems. *Nature Communications*, 11(1), 1175. Article 1175.  
<https://doi.org/10.1038/s41467-020-15029-x>

#### Hawliau Cyffredinol / General rights

Copyright and moral rights for the publications made accessible in the public portal are retained by the authors and/or other copyright owners and it is a condition of accessing publications that users recognise and abide by the legal requirements associated with these rights.

- Users may download and print one copy of any publication from the public portal for the purpose of private study or research.
- You may not further distribute the material or use it for any profit-making activity or commercial gain
- You may freely distribute the URL identifying the publication in the public portal ?

#### Take down policy

If you believe that this document breaches copyright please contact us providing details, and we will remove access to the work immediately and investigate your claim.

# 1 Regime shifts occur disproportionately 2 faster in larger ecosystems

3  
4 **Gregory S. Cooper<sup>1†</sup>, Simon Willcock<sup>2†</sup> and John A. Dearing<sup>3\*</sup>**

5  
6 <sup>1</sup> Centre for Development, Environment and Policy (CeDEP), School of Oriental and African Studies,  
7 University of London, WC1H 0XG, United Kingdom

8 <sup>2</sup> School of Natural Sciences, Bangor University, Bangor, LL57 2DG, United Kingdom

9 <sup>3</sup> Geography and Environmental Science, University of Southampton, Southampton, SO17 1BJ,  
10 United Kingdom

11

12 \*Corresponding author: John A. Dearing, [J.Dearing@soton.ac.uk](mailto:J.Dearing@soton.ac.uk)

13 † these authors contributed equally to this work

14

## 15 **Abstract**

16 Regime shifts can abruptly affect hydrological, climatic and terrestrial systems, leading to degraded  
17 ecosystems and impoverished societies. While the frequency of regime shifts is predicted to increase,  
18 the fundamental relationships between the spatial-temporal scales of shifts and their underlying  
19 mechanisms are poorly understood. Here we analyse empirical data from terrestrial (n=4), marine  
20 (n=25) and freshwater (n=13) environments and show positive sub-linear empirical relationships  
21 between the size and shift duration of systems. Each additional unit area of an ecosystem provides  
22 an increasingly smaller unit of time taken for that system to collapse, meaning that large systems  
23 tend to shift more slowly than small systems but disproportionately faster. We substantiate these  
24 findings with five computational models that reveal the importance of system structure in  
25 controlling shift duration. The findings imply that shifts in Earth ecosystems occur over ‘human’  
26 timescales of years and decades, meaning the collapse of large vulnerable ecosystems, such as the  
27 Amazon rainforest and Caribbean coral reefs, may take only a few decades once triggered.

28

## 29 **Introduction**

30 Anthropogenic activities are dependent upon the persistence of various biophysical conditions, such  
31 as soil fertility, freshwater availability and stable fish populations<sup>1</sup>. However, regime shifts can cause  
32 significant negative impacts on Earth's contemporary social-ecological systems<sup>2</sup>. For example,  
33 marine fishery collapses over the past fifty years have degraded continental-scale food securities  
34 and economic opportunities<sup>3,4</sup>. Such shifts also exist at local scales, with coastal lagoons, estuaries  
35 and freshwater environments susceptible to significant declines in ecosystem conditions and socio-  
36 economic productivity<sup>5</sup>. Here, we conceptualise regime shifts as large, persistent, and often  
37 unexpected changes in relatively stable ecosystems<sup>6,7</sup>, which may (or may not) be driven by  
38 reinforcing feedback loops beyond 'tipping points'<sup>8,9</sup>. From this definition, we consider shift duration  
39 to be the time taken to transition to a stable but functionally different system state<sup>8</sup>.

40         Problematically for their governance, regimes shifts are traditionally viewed as abrupt  
41 relative to the temporal scales of the initial and resulting regimes<sup>4,10</sup>. Regime shifts are often  
42 associated with a preceding decline in resilience, associated with the inability of system structures to  
43 maintain stability under stress<sup>11,12</sup>. However, the current suite of resilience metrics currently lack  
44 robust cross-system transferability<sup>13</sup> and the general sparsity of quantitative information on regime  
45 shifts further complicates their prediction and governance<sup>9</sup>. With the frequency of regime shifts  
46 predicted to increase in association with climate change and environmental degradation<sup>14</sup>,  
47 developing the general understanding into the spatial and temporal dynamics of shifts would help to:  
48 anticipate the nature and timing of potential impacts; improve understanding into the role of system  
49 structure on resilience; and identify sizes of 'window of opportunities'<sup>15</sup> to implement adaptive  
50 management to reduce socio-economic and ecological damage.

51         We use network science to inform two hypotheses that link the speed of a regime shift to  
52 the size and structure of the system (Fig. 1). We hypothesize that larger systems (as  
53 measured by area) should intuitively take longer in absolute terms to shift between alternate  
54 regimes due to time-distance relationships, the diffusion of stresses and built-in time-lags. However,

55 systems vary in terms of the speed by which a stressor may transmit through a system, from fluid,  
56 highly connected atmospheres and water bodies to less fluid terrestrial systems where physical  
57 infrastructure, like soil horizons and river channels, may reduce transmission speeds across the  
58 whole system. In turn, modularity, or the relative number of independent (i.e. unconnected) sub-  
59 systems, is a structural attribute that potentially slows cascading effects once a transition has been  
60 triggered (i.e. many independent smaller systems tip cumulatively more slowly than a single larger  
61 system of the same total size; Fig. 1)<sup>16</sup>.

62 Hierarchical, self-organized biological systems and ecosystems possess attributes which  
63 scale sub-linearly with system size through the limits of energy dissipation, including tree branching  
64 or blood vessel networks<sup>17</sup>, and production or predator-prey biomass<sup>18</sup>. In terms of network  
65 connectivity, it is known that heterogenous, hierarchical systems are resilient to random failure but  
66 vulnerable to targeted attack or failure of keystone nodes<sup>19</sup>. It follows that such systems should  
67 cascade relatively quickly once the keystone nodes are damaged or extirpated. In mechanistic terms,  
68 the breakdown of organisation during a regime shift might be expected to track the same sub-linear  
69 scaling trend. Thus, we also hypothesise that the size-duration relationship will tend to display a sub-  
70 linear power law relationship – indicating relatively faster regime shifts for large systems.

71 To test these two hypotheses, we first compile empirical data on real-world ecosystem shifts  
72 from scientific publications, institutional reports and online collations such as the Regime Shifts  
73 Database<sup>7</sup> and the Threshold Database<sup>20</sup> (see Methods and Supplementary Table 1). Each of the 42  
74 observed shifts meet various criteria for inclusion (see Methods) based upon the characteristics of  
75 the shift from one regime to another and our ability to precisely and reliably estimate the spatial and  
76 temporal extents of the shifts. Modelling has revealed the likely type of regime shift in some cases  
77 (i.e. the presence of a tipping point, critical transition or hysteresis<sup>2,8</sup>), but we make no assumptions  
78 about the reversibility of each shift. While we recognise that our empirical sample is not exhaustive,  
79 the dataset covers a variety of biophysical systems across seven orders of spatial magnitude, three  
80 orders of temporal magnitude, five continents and three environmental settings.

81 We substantiate these real-world relationships with five freely available computational  
82 models: Wolf-Sheep Predation (WSP)<sup>21</sup>; Game of Life (GoL)<sup>22</sup>, Language Change (LC)<sup>23,24</sup>, Lake Chilika  
83 fishery (CHL)<sup>25</sup> and Spatial Heterogeneity (SH)<sup>2</sup> to substantiate the potential spatial characteristics  
84 behind the empirical relationships (Table 1 and Methods). A total of twelve ecological modelling  
85 experiments were designed to unravel the hypothesised effects of scale, fluidity, modularity, and the  
86 heterogeneity of connections on the duration of regime shifts (Table 1 and Fig. 1). In particular, we  
87 selected models with dynamic variables that are capable of shifting from one state to another, and  
88 which we could control explicitly for either system size or system structure in multiple runs (see  
89 Methods). We selected models that capture both reversible, non-catastrophic shifts (e.g. WSP) and  
90 catastrophic shifts where reversibility demands overcoming hysteresis<sup>26</sup> (e.g. fishery collapse in the  
91 CHL model). Moreover, these models are all freely available making the experiments reproducible  
92 with the model details and NetLogo codes provided in Supplementary Tables 3-7.

93 We find positive sub-linear empirical relationships between the size and shift duration of  
94 systems for both the empirical and modelled data. This indicates that large systems tend to shift  
95 more slowly than small systems but faster per unit area. Using this relationship, we predict that the  
96 collapse of large vulnerable ecosystems (e.g. the Amazon rainforest) may take only a few decades  
97 once triggered.

98

## 99 **Results and discussion**

### 100 **Empirical data**

101 As hypothesised, the real-world records show a positive association between system area and shift  
102 duration (Fig. 2), implying that shifts in larger systems, once triggered, take longer to reach a new  
103 regime. The overarching relationship is also sub-linear (Fig. 2), remaining statistically significant both  
104 with (slope = 0.221,  $R^2 = 0.491$ ,  $p < 0.001$ ,  $df = 40$ ) and without the Sahara record (slope = 0.190,  $R^2 =$   
105 0.423,  $p < 0.001$ ,  $df = 39$ ).

106 We tested the robustness of this relationship with two sensitivity analysis experiments (as well as  
107 the plotting of generalised linear models, which can be found in Supplementary Table 1): (i) where  
108 alternative datasets were generated ( $n = 42$ ), with one record from the original dataset removed in  
109 each (Supplementary Table 2), and (ii) using a Monte Carlo style approach where each of the original  
110 42 records were given random error magnitudes between 50% and 150% of their original values  
111 across 5,000 probabilistic simulations (see Methods and Supplementary Figs 5-6). In the first  
112 sensitivity experiment, all of the 42 alternative models were found to have positive and sub-linear  
113 relationships between system size and shift duration (all significant to  $p < 0.001$  level;  
114 Supplementary Table 2). Moreover, the original empirical model (Fig. 2) is found to be most sensitive  
115 to the record of the Sahara Desert; however, the removal of its record leads to a 14% decrease in the  
116 'b-coefficient/slope term', making the new model more sub-linear. In the second sensitivity  
117 experiment, all 5000 simulations exhibited positive and sub-linear relationships between system size  
118 and shift duration (all significant to  $p < 0.001$  level; Supplementary Fig. 6). Therefore, we infer that  
119 the power-law relationship is robust (Fig. 2), and not dependent on any one datapoint nor the  
120 assumption that the empirical dataset has unreasonably narrow error bounds. The robust sub-  
121 linear power law relationships suggest that although there is an overarching positive association  
122 between area and shift duration, larger systems shift comparatively quickly relative to their size. In  
123 other words, the change in shift duration slows down as system size increases, implying that the  
124 trend line asymptotes towards some theoretical maximum shift time for Earth's ecosystems. A  
125 similar result is observed for estimated system volumes (Supplementary Fig. 3) and additional  
126 empirical data are unlikely to fill the size-duration space (Fig. 2) to the extent that the broad  
127 statistical relationships are overturned; instead, uncertainty surrounding this relationship would  
128 likely be reduced.

129 The empirical results provide first order estimations for the shift durations of iconic  
130 ecosystems like The Amazon rainforest and Caribbean coral reefs. The empirical model (Fig. 2)  
131 estimates that an ecosystem the size of the Amazon ( $\sim 5.5$ -million  $\text{km}^2$ ) will shift over 49 years (95%

132 confidence interval [CI]: 10-260 years), which is broadly in line with the multidecadal shift durations  
133 projected by expert judgement<sup>9</sup> and process-based models<sup>14,27</sup>. Worryingly, recent plot inventories  
134 from the Amazon show a declining rate of carbon sequestration<sup>28</sup>, and there is growing evidence  
135 that further deforestation and degradation of the feedback between moisture formation and  
136 vegetation coverage may lead to a system-wide tipping point as soon as 2021<sup>29,30</sup>. For a system the  
137 size of the Caribbean coral reefs ( $\sim 20,000 \text{ km}^2$ )<sup>31</sup>, the empirical model estimates a 15 year period (95%  
138 CI: 5-50 years) to collapse once triggered. The decadal timescales are coherent with the observations  
139 that coral cover across the Caribbean declined by 80% from 1977 to 2001<sup>32</sup> and may completely  
140 disappear by 2035<sup>33</sup>, depending on rates of further overfishing, climate change and ocean  
141 acidification. While the uncertainty bounds around the mean estimates must be acknowledged,  
142 these two collapses remain within 'human' timescales of years and decades (stretching to centuries  
143 at the edges of the 95% confidence interval).

144

#### 145 **Model results**

146 First, we analyse the direct effects of system size on shift duration and whether the change in regime  
147 shift duration generally increases (super-linear) or decreases (sub-linear) with the change in spatial  
148 dimension (Fig. 3). Here, the modelled results are consistent with our empirical findings and show  
149 that shift duration is positively and sub-linearly associated with increasing system size as measured  
150 by system area (WSP-1.1, GoL-2.1 and CHL-4) and carrying capacity (SH-5.1) (Fig 3;

151 slope term,  $b < 1$ ). The exception is where system size is measured by the number of system nodes  
152 (LC-3.1) and then shift duration scales super-linearly (slope  $> 1$ ).

153 Second, we compare the model outputs with their different structures to gain insight into  
154 why the sub-linear relationships exist. Consistent with our hypothesis, we find that shift duration is  
155 negatively correlated with system fluidity in both the GoL (GoL-2.3) and the SH (SH-5.2) models (Fig  
156 3). We also find that shift duration is positively associated with system modularity (WSP-1.1 and  
157 GoL-2.2), where more modular (i.e. less fluid) systems are slower to shift from one regime to  
158 another. Moreover, heterogeneously wired systems (i.e. those with keystone nodes) tend to require  
159 less time to transition once a shift has been triggered (LC-3.3).

160 The two structural experiments that are inconsistent with our initial hypotheses are the WSP  
161 fluidity (WSP-1.3) and LC connections (LC-3.2) simulations as we find these had no effect on shift  
162 duration. Therefore, we hypothesise that the GoL fluidity experiment (GoL-2.3) suggests that spatial  
163 fluidity better influences regime shift duration when the direction of stress transmission is less  
164 restricted; for example, switching between a von Neumann four-direction neighbourhood<sup>34</sup> to a  
165 Moore eight-direction neighbourhood<sup>34</sup> (see Methods). In contrast, the insignificant WSP fluidity  
166 result suggests that the ability of a stressor to move further through a system is less important than  
167 the subsequent target of the stress because the stressor may just attack a resistant or unimportant  
168 part of a system in a distant location (e.g. a non-keystone node). This hypothesis is also supported  
169 empirically, though data are sparse (Supplementary Fig. 4), with the four terrestrial systems (less  
170 fluid) plotting along a steeper line than other systems containing freshwater and marine transitions  
171 (more fluid). In any case, system fluidity appears to be subordinate to system size in controlling shift  
172 duration, with the size versus time relationship remaining significant and positive across all five  
173 models.

174

175 **Mechanisms in real and model systems**

176 The empirical and modelled findings point to there being a fundamental mechanism in ecosystems  
177 that links physical size, structure and speed of failure. In terms of size and structure, the large body  
178 of ecological research on area-diversity relationships<sup>35,36</sup> allows us to assume that the self-  
179 organizational processes which create increasingly complex structures with, for example, more  
180 trophic levels, higher species richness or more sub-system modules, are strongly limited by space. It  
181 follows that large ecosystems will show disproportionately more complexity than small ecosystems.  
182 In that case, a recent analysis of coupled regime shifts<sup>37</sup> helps to identify two possible reasons why  
183 disproportionately high complexity in large ecosystems may instil resilience against a system  
184 reaching a regime shift, but once triggered provides favourable structures for failure: (1) there is a  
185 greater probability in larger systems that a 'shared' driver initiates synchronous failure in sub-system  
186 'modules' at more than one location; and (2) there is a greater probability that the weak feedback  
187 mechanisms that maintain the stability of large, mature systems will be dominated by the  
188 emergence of stronger, 'hidden' feedbacks that progressively raise the probability that the failure of  
189 one sub-system will affect the stability of a neighbour. These two points are illustrated, respectively,  
190 by current concerns about the effects of disparate fires on the long-term resilience of the Amazon  
191 forest to climate change<sup>25</sup>; and the rapid spread of recent (2019-20) bush fires in SW Australia  
192 caused by existing fires igniting further fires<sup>38</sup>.

193

194 The structural experiments support these ideas. From a network perspective, the LC model shows  
195 that systems with heterogenous connections (Fig. 3) generally shift more rapidly than networks with  
196 relatively homogenous numbers of connections per node. This reflects the idea of 'keystone' nodes  
197 (Supplementary Fig. 8) which once flipped (e.g. 'black' to 'white') help to transmit stresses rapidly  
198 across the network, an interpretation that is consistent with the greater vulnerability of scale-free  
199 networks to a targeted attack on keystone nodes<sup>19</sup>. As expected, large systems of all kinds transmit  
200 stresses more slowly through greater distances, with some empirical (Supplementary Fig. 4) and  
201 modelled evidence suggesting fluid systems tend to transition more quickly (Fig. 3). However, this

202 relationship is also sub-linear, implying a law of diminishing returns with each increase in system  
203 fluidity resulting in a disproportionately smaller decrease in shift duration. Therefore, whilst the  
204 general negative association between fluidity and shift duration reflects the tendency for relatively  
205 resilient locations to emerge within system structures with lower connectiveness<sup>16</sup>, more fluid  
206 systems (i.e. less modular) may lead to longer regime shift durations than would be otherwise  
207 expected under linear scaling. In other words, the ability of increasing fluidity to inhibit the rate of  
208 overall system transitioning may gradually weaken as the connectivity increases.

209           These findings on ecosystems invite a prediction about scale and shift duration in social and  
210 economic systems. It has been theorised that the difference between sub-linear and super-linear  
211 scaling with size is linked to the different controlling effects of system structure in ecosystems versus  
212 system interactions in social systems<sup>17</sup>. This would imply that, in contrast to ecosystems, the  
213 collapse of social or economic systems (e.g. inter-bank trading) should scale super-linearly with  
214 disproportionately *slower* shift durations. Consistent with this, the empirical power law relationship  
215 identified here becomes less sub-linear once social collapses are included (Supplementary Fig. 2);  
216 however, too few empirical data currently exist to fully and robustly explore this hypothesis.

217

### 218 **Implications for governance**

219 Ultimately, our findings have multiple implications for the governance of real-world systems. First,  
220 from local to sub-continental scales ( $10^0$ - $10^6$  km<sup>2</sup>), we must prepare for regime shifts in any natural  
221 system to occur over the 'human' timescales of years and decades, rather than multi-generational  
222 timescales of centuries and millennia. Second, the apparent long-term stability of the largest, least  
223 disturbed ecosystems is a deceptive guide to the potential speed of their collapse. Therefore, the  
224 self-organising mechanisms (e.g. modularity) that help to instil systems with resilience prior to a  
225 tipping point may have limited ability to control the rate of collapse once a shift has been triggered.  
226 Third, homogenously connected systems shift relatively less quickly, meaning that ecosystems that  
227 are already disturbed but stabilised, or those that are engineered, may be relatively slower to

228 collapse because of the lack of vulnerable modular structures. Thus, although shifts in  
229 agroecosystems are expected due to climate change<sup>39</sup>, their relatively slow transitions may offer  
230 vital time for adaptation. Fourth, the ‘window of opportunity’<sup>15</sup> open to divert unsustainable system  
231 trajectories is comparatively short for relatively small systems, meaning contingency plans should be  
232 formulated in advance and ready to implement across localised systems recognised to be heading  
233 towards the brink.

234 The exponentially increasing global trends of many social and biophysical variables over the  
235 past 65 years are widely viewed as unsustainable<sup>40</sup>. Along with the evidence for increasingly strong  
236 reinforcing feedbacks, interactions and couplings between variables<sup>37,41,42</sup>, there is growing  
237 awareness around the heightened risk of current anthropogenic activities triggering sub-global  
238 regime shifts<sup>14</sup>. Combined with the findings presented here, humanity now needs to prepare for  
239 changes in ecosystems that are faster than we previously envisaged through our traditional linear  
240 view of the world, including across Earth’s largest and most iconic ecosystems – and the social-  
241 ecological systems that they support.

242

## 243 **Methods**

### 244 **Literature search strategy, case-study qualifications and dataset**

245 The literature search used three electronic databases, namely the University of Southampton’s  
246 DelphiS interface, Web of Science and Google Scholar. Prospective case-studies were recognised by  
247 individual cases or combinations of the following key terms appearing within either the article title  
248 or abstract: regime shift, critical shifts, shift, abrupt shift, threshold change, tipping point, stark shift,  
249 abrupt change, human-natural system, ecosystem, ecological, social-ecological, ecosystem,  
250 irreversible, landscape, environment.

251 The literature search was carried out from February to August 2018. Date limits were not  
252 imposed on the year of publication. In addition, case-studies from both the Regime Shift Database<sup>7</sup>  
253 of the Stockholm Resilience Centre and the Threshold Database<sup>20</sup> of the Resilience Alliance were  
254 considered for inclusion. Each potential case-study, including the social systems included in  
255 Supplementary Fig. 2, had to then meet the following three-part criteria to be included in the  
256 empirical dataset of this study:

- 257 1. For inclusion based upon the characteristics of the regime shift, each case-study must  
258 exhibit:
  - 259 a) A demonstrated/observed state change in a real-world environment, rather than just  
260 hypothesised or modelled.

- 261 b) Recognisable and clearly defined alternate states, consistent with common definitions,  
262 including both quantitative (e.g. ecosystem service availability) and quantitative (e.g.  
263 structural change) indicators.
- 264 c) Driver(s) of change that are beyond natural and/seasonal variations/cycles.
- 265 d) Irreversibility over the temporal horizon of the original study.
- 266 e) Or, if reversed, human-led remediation efforts (e.g. artificially manipulating water  
267 quality) were completed over the course of the study.
- 268
- 269 2. In order to confidently and consistently measure the spatial extent (and depth) of shifts, the  
270 following steps were applied:
- 271 a) Use regime shift area (and depth where applicable) directly quoted in the case study  
272 publication.
- 273 b) Ascertain whether the shift occurred across the whole system or subsystem of wider  
274 geographical entity, then:
- 275 i. Consult 'Locational Information/Case Study/Methodology' sections of scientific  
276 publications to find quoted area of shift.
- 277 ii. If shift occurred across entire system, we searched within related scientific  
278 publications to find extent (and depth) of system.
- 279 iii. Widening the search to institutional literature, such as maritime management  
280 reports.
- 281
- 282 3. In order to confidently and consistently measure the temporal scale of shifts (i.e. the time  
283 taken to transition to a stable but functionally different system state), the literature either:
- 284 a) Directly quoted the shift duration in text.
- 285 b) Explicitly depicted shift duration in a time-series of system conditions, with the  
286 significant deviation from the preceding regime flagged.
- 287 c) Visually estimated shift duration from a time series of system conditions. To remain  
288 consistent, the tipping point was always identified by the first sign of significant  
289 divergence from the preceding trend.

290 After applying the above qualifications, the final dataset (Supplementary Table 1) includes  
291 42 regime shifts observed in nature (25 marine, 13 freshwater and 4 terrestrial).

292

### 293 **Sensitivity analysis of empirical results**

294 The empirical dataset suggests that there is an overarching positive association between system  
295 area and shift duration, and that larger systems tend to shift comparatively quickly relative to their  
296 size. However, it is reasonable to ask questions around the uncertainty of this result. Therefore, we  
297 investigate the extent to which the sub-linear trend is (i) dependent on any one data point in the  
298 empirical dataset, and (ii) affected by uncertainties within the empirical dataset. Regarding point (i),  
299 we created 42 new empirical datasets, each with one of the empirical records removed. We fitted  
300 power-law relationships to each of the new 42 datasets (each with 41 empirical records) and  
301 assessed the degree to which removing any one empirical record impacted the production of a  
302 significant, sub-linear association between system area and shift duration. We undertook a simple  
303 Monte Carlo analysis to investigate point (ii). For each of the 42 empirical records, 5,000 random  
304 error terms were generated, converting the shift durations to values between 50-150% of their  
305 original values. The resulting error ranges are graphically represented in Supplementary Fig. 5. Error  
306 terms were only applied to the shift durations, as confidence in the system area values is relatively  
307 high (Supplementary Table 1). From here, we fitted power-law regression models through each of  
308 the 5,000 new models and recorded the resulting slope and significance coefficients. All analyses  
309 were conducted using the statistical software R<sup>43</sup>.

310

### 311 **Model selection strategy**

- 312 The model search was carried out from February 2018 to February 2019, during which we identified  
 313 models that reflected the characteristics of the empirical regime shifts data obtained.
- 314 1. For inclusion based upon the characteristics of the regime shift, each model must exhibit:
    - 315 a) A state change.
    - 316 b) Recognisable and clearly defined alternate states, consistent with common  
 317 definitions, including both quantitative (e.g. ecosystem service availability) and  
 318 quantitative (e.g. structural change) indicators.
    - 319 c) Variables acting as driver(s) of change.
  - 320 2. In order to confidently and consistently measure the temporal scale of shifts, the model  
 321 either:
    - 322 a) Explicitly depicted shift duration in a time-series of system conditions, starting in an  
 323 unstable state, where the start of the shift is assumed to be the start of the model  
 324 run.
    - 325 b) Started in a stable state, from which shift duration could be estimated from a time  
 326 series of system conditions. To remain consistent, the tipping point was always  
 327 identified by the first sign of significant divergence from the preceding trend (see  
 328 'Identifying regime shift durations of modelled time-series' for more details below).
  - 329 3. In order to investigate the impact of system characteristics, the model either:
    - 330 a) Allowed for variation in system size.
    - 331 b) Allowed for variation in metrics of system fluidity or connectedness.
  - 332 4. Finally, in accordance with FAIR principles<sup>44</sup>, models were required to be open-access.

333 After applying the above qualifications, we obtained five models of regime shifts that are findable,  
 334 accessible and reusable as well as being comparable to our empirical data. Of these models, two are  
 335 known to illustrate tipping points and hysteresis (CHL and SH models). The models are described  
 336 below.

337

338 **The Wolf-Sheep Predation (WSP) agent-based model**

339 The WSP model explores the stability of predator-prey relationships<sup>21</sup>. The construction of this  
 340 model is described in two principle articles<sup>45,46</sup>. In our investigation, we used a variation of the model  
 341 which includes grass in addition to wolves and sheep. Both wolves and sheep are randomly  
 342 generated and move randomly through a landscape. Each step, costs both animals in terms of  
 343 energy; wolves must eat sheep and sheep must eat grass in order to replenish their energy.  
 344 Therefore, any animals that run out of energy die. Once grass has been eaten, it will regrow after a  
 345 fixed number of model steps. Finally, every animal has a fixed probability of reproducing at each  
 346 time step. This model is freely available within the NetLogo software<sup>47</sup> and the default values for the  
 347 model variables are shown in Supplementary Table 3. The WSP model outlined above is sometimes  
 348 stable<sup>21</sup>, but can be made unstable by varying the grass regrowth time. Once the model is unstable,  
 349 it can be observed to go through three possible regime shifts (Supplementary Fig. 7): (1) the  
 350 extinction of wolves, (2) the extinction of sheep, (3) the progression of the landscape to full  
 351 grassland, which with no grazers present, could lead to succession towards another ecosystem state.  
 352 By altering specific variables and then destabilising the WSP model we were able to investigate the  
 353 impact of those variables on the duration of the regime shifts. The variables we investigated using  
 354 the WSP model were system area, module size, and system fluidity (Table 1). To investigate the  
 355 impact of the area of the landscape on the duration of the regime shift, we increased the length and  
 356 width of the landscape by two pixels at a time between 1 and 100, whilst maintaining constant  
 357 starting densities of both wolves and sheep (Supplementary Table 3). To ensure unstable systems,  
 358 the reproduction rates of sheep were altered to a constant of 7% and grass regrowth time was  
 359 varied from 1 to 100. Using the 'BehaviorSpace' tool within Netlogo<sup>47</sup> every variation of this model  
 360 was run for 5,000 time steps, unless all three regime shifts occurred prior to this. This process  
 361 resulted in 260,100 model runs. To investigate the impact of the size of modules within the  
 362 landscape on the duration of the regime shift, we varied the height of the landscape between 2, 5,

363 10, 20, 50, and 100 cells. Here we again maintained constant starting densities of both wolves and  
364 sheep, but summed model runs together so that world size was consistently 100 x 100 pixels  
365 (Supplementary Table 4). To ensure unstable systems, the reproduction rates of sheep were altered  
366 to a constant of 7% and grass regrowth time was varied from 1 to 100. As per the world size  
367 experiment, every variation of this model was run for 5,000 time steps, unless all three regime shifts  
368 occurred prior to this. This process was repeated 100 times, resulting in 930,000 model runs. To  
369 investigate the impact of the system fluidity on the duration of the regime shift, we varied the  
370 mobility of the animals between 1 and 100, whilst maintaining a constant landscape size of 100 x  
371 100 pixels (Supplementary Table 4). To ensure unstable systems, the reproduction rates of sheep  
372 were altered to a constant of 7% and grass regrowth time was varied from 1 to 100. Every variation  
373 of this model was run for 5,000 time steps, unless all three regime shifts occurred prior to this. This  
374 process resulted in 10,000 model runs. The GoL model can be obtained from the following URL:  
375 <https://ccl.northwestern.edu/netlogo/models/WolfSheepPredation>  
376

### 377 **Game of Life (GoL) cellular automaton model**

378 In the two-dimensional GoL each cell can be either one of two possible states: 'alive' or 'dead'. At  
379 every time step, each cell checks the state of itself and its neighbours, and then sets itself as either  
380 alive or dead based on its neighbours' states. This model is freely available within the NetLogo  
381 software<sup>22</sup> and the default values for the model variables are shown in Table S5. The GoL model  
382 outlined above is inherently unstable when an initial density of 35% is used (i.e. the system begins to  
383 shift from the initial state to the alternative state as soon as the model run begins). Upon starting  
384 the model at this density, the number of 'alive' cells decreases until a stable state is reached. Thus,  
385 the system can only be observed to go through one possible regime shift: from an unstable state  
386 with both alive and dead cells to an alternate stable state in which either all cells are dead, or a  
387 stable mixed state has been reached. By altering specific variables we were able to investigate the  
388 impact of those variables on the duration of the regime shift, starting from an unstable state. The  
389 variables we investigated using the GoL were system size, module size, and system fluidity (Table 1).  
390 In order to determine when stability occurred, we inserted a new stop function (Supplementary  
391 Note 3) which would stop the model if the number of living cells did not change for 100 time steps.  
392 To investigate the impact of the size of the landscape on the duration of the regime shift, we  
393 increased the length and width of the landscape by two pixels at a time between 1 and 100, whilst  
394 maintaining consistent starting densities of both alive and dead cells (Supplementary Table 5). To  
395 ensure unstable systems, the initial density was set to 35%. Using the 'BehaviorSpace' tool within  
396 Netlogo, every variation of this model was run for 5,000 time steps, unless a stable state was  
397 reached prior to this. This process resulted in 260,100 model runs. To investigate the impact of the  
398 size of modules within the landscape on the duration of the regime shift, we varied the height of the  
399 landscape between 2, 5, 10, 20, 50, or 100, again whilst maintaining consistent starting densities of  
400 both alive and dead cells, but summed model runs together so that word size was consistently 100 x  
401 100 pixels (Supplementary Table 5). To ensure unstable systems the initial density was set to 35%.  
402 Every variation of this model was run for 5,000 time steps, unless a stable state was reached prior to  
403 this. This process was repeated 100 times, resulting in 930,000 model runs. To investigate the impact  
404 of the system fluidity of the landscape on the duration of the regime shift, we varied the number of  
405 neighbours each cell considered between 4 (i.e. von Neumann neighbourhood<sup>34</sup>) and 8 (i.e. Moore  
406 neighbourhood<sup>34</sup>), whilst maintaining a constant landscape size of 100 x 100 pixels and a constant  
407 proportion for the decisions to 'die' (Supplementary Table 5). To do this, we further adapted the  
408 standard GoL code, updating the 'to go' function to include both possible neighbour combinations  
409 (Supplementary Note 3). To ensure unstable systems, the initial density was set to 35%. Every  
410 variation of this model was run for 5,000 time steps, unless a stable state was reached prior to this.  
411 This process was repeated 100 times, resulting in 200 model runs. The GoL model can be obtained  
412 from the following URL: <https://ccl.northwestern.edu/netlogo/models/Life>  
413

#### 414 **Language Change (LC) network model**

415 The LC model explores how the structure of social networks can affect the course of language  
416 change<sup>23,24</sup> (Supplementary Fig. 8). In our investigation, we used a variation of the model (termed  
417 ‘individual’) in which individuals can only access one language at a time. Each time-step, individuals  
418 choose one of their neighbours randomly and then adopt that neighbour’s language (Language 1 or  
419 Language 2). This model is freely available within the NetLogo software<sup>47</sup> and the default values for  
420 the model variables are shown in Supplementary Table 6. The LC model outlined above is inherently  
421 unstable. Language 1 is created as dominant and cannot be lost once adopted<sup>23</sup>. Thus, the system  
422 can only be observed to go through one possible regime shift: from a mixed state with two  
423 languages to an alternate state whereby language 1 has become saturated in the population  
424 (Supplementary Fig. 8). By altering specific variables, we were able to investigate the impact of those  
425 variables on the duration of the regime shift, starting from an unstable state. The variables we  
426 investigated using the LC model were number of connections, number of nodes and network  
427 connection heterogeneity (Table 1). To investigate the impact of the number of connections in a  
428 network on the duration of the regime shift, we varied the number of connections between 99 and  
429 4,500 (Supplementary Table 6). In order to do this, the number of connections was added as a global  
430 variable and the code to create the network was altered to ensure the number of connections  
431 between nodes was equal to this user-defined value (Supplementary Note 4). Using the  
432 ‘BehaviorSpace’ tool within Netlogo, every variation of this model was run for 5,000 time steps,  
433 unless the regime shift occurred prior to this. This process was repeated 100 times, totalling 440,200  
434 model runs. To investigate the impact of the number of nodes in a network on the duration of the  
435 regime shift, we varied the number of nodes between 3 and 1,000 (Supplementary Table 6). The  
436 number of connections was set to one but would default to the number of nodes minus one to  
437 ensure all nodes were connected. Every variation of this model was run for 5,000 time steps, unless  
438 the regime shift occurred prior to this. This process was repeated 100 times, totalling 99,800 model  
439 runs. Instead of re-running the LC model to specifically investigate the impact of network connection  
440 heterogeneity on the duration of regime shifts, we maximised computational efficiency by analysing  
441 network heterogeneity in the systems used to investigate the number of connections. During the  
442 above LC model experiments, we recorded the standard deviation of the number of connections of  
443 each link; acting as an appropriate measure of the heterogeneity of the connection distributions as  
444 the underlying distribution is normal (Gaussian; Fig. S8). The LC model can be obtained from the  
445 following URL: <https://ccl.northwestern.edu/netlogo/models/LanguageChange>  
446

#### 447 **Lake Chilika fishery (CHL) system dynamics model**

448 The CHL model<sup>25</sup> was built to investigate the future social-ecological sustainability of the Chilika  
449 lagoon – Asia’s largest brackish water ecosystem – located in Odisha, India. Essentially, the model  
450 simulates the coupled effects of various biophysical and socioeconomic pressures on the fish stock.  
451 As a system dynamics model, the key dynamics of the social-ecological system are represented as  
452 stocks (e.g. fish population, lake water sediment and aquatic vegetation), flows (e.g. freshwater and  
453 climatic inputs, fish births and deaths) and feedbacks (e.g. fishery intensification) which all evolve  
454 over time. Each model time-step equals one month, although outputs are generally aggregated to  
455 the annual resolution to improve visualisation. Here, simulations are run for 1524 timesteps,  
456 equalling 127 years (i.e. the period from 1973-2099). In the original model<sup>25</sup>, the model simulates  
457 four socioeconomic stresses on the fish population: (i) the number of fishers able to generate their  
458 livelihood from the fishery is related to a simple carrying capacity, based on the economic revenue  
459 of the fish catch, the average income of each fleet (i.e. traditional and motorised) and the minimum  
460 cost to fish; (ii) relatively affluent traditional fishers may switch from traditional wind-assisted sailing  
461 boats to relatively fish catch intensive motorboats; (iii) the number of days fished each month is  
462 proportional to the underlying density of the fish population; (iv) whilst the acceptance of juvenile  
463 catch increases during stock declines to compensate for lost fishing days. The original model also  
464 captures three biophysical pressures on the fish population: (i) the effect of tidal outlet

465 sedimentation and closure on the migration of fish to and from the Bay of Bengal, with 70% of the  
466 fish stock undertaking this migration pathway each year to complete their natural breeding cycles;  
467 (ii) the effects of lake water salinity, temperature and dissolved oxygen concentration on the survival  
468 rate of juvenile fish per unit time; (iii) the growth of surface water aquatic vegetation which provides  
469 refuge from fishery activities. The model also simulates the effects of alternative governance  
470 options, including the implementation of fishing bans and the frequency of tidal outlet maintenance  
471 (i.e. removal of accumulated sediment). The model is aspatial, as per the vast of system dynamics  
472 models. However, the model does simulate the effect of lake area on the growth of aquatic  
473 vegetation and the volume of rainfall falling directly onto the lake – with subsequent impacts on the  
474 salinity of the lake water and the accumulation of lacustrine sediment (i.e. larger area leads to higher  
475 direct rainfall inputs, leading to greater flushing of sediment from the lagoon). Therefore, to model  
476 the direct association between lake area and the duration of transition, we turn off all  
477 socioeconomic pressures (i.e. set fish catch from both fleets equal to zero). In turn, we vary the  
478 parameter named 'Chilika area km<sup>2</sup>' between 500 km<sup>2</sup> and 10,000 km<sup>2</sup> (i.e. 50-1000% of the original  
479 lake value). The model is run for 5000 simulations in the sensitivity analysis mode, sampling a  
480 different lake area between the minimum and maximum area limits per simulation. Tidal outlet  
481 maintenance is turned off, meaning the lacustrine sediment is allowed to accumulate naturally.  
482 Similar to the WSP model (Supplementary Table 3), the model may remain stable across the  
483 simulation horizon. Therefore, the breakpoint function<sup>48</sup> is used to detect the onset of the shift and  
484 the end of the shift is flagged once the fish population falls beneath 1% of the fish population  
485 recorded at the start of the simulation (Supplementary Fig. 10). The model exhibits fold bifurcation  
486 behaviour and hysteresis; for example, in Supplementary Fig. 11, whereby attempts to recover the  
487 collapsed fish population require the stressor (i.e. lake salinity, which is a proxy for lake  
488 sedimentation and tidal outlet closure) to be reversed back past the point that caused the original  
489 transition. The model is available on reasonable request from the authors of the original study<sup>25</sup>.

490

#### 491 **Spatial Heterogeneity (SH) model**

492 The SH model is an illustration of how spatial structure can affect the potential of systems to  
493 oscillate, particularly how stabilization can arise through spatial heterogeneity<sup>2</sup>. The SH model is  
494 known to show Hopf bifurcations<sup>2</sup>. The model uses predator-prey relationships to represent the  
495 interaction between zooplankton and algae co-existing within a lake but simplifies the spatial  
496 processes by considering zooplankton to be situated in one part of the lake, while algae are present  
497 throughout (Supplementary Fig. 12). Thus, in one compartment (A1) zooplankton graze the local  
498 population of algae, but the algae within the other compartment (A2) are predation free. The model  
499 experiments observe the shift to a state where the zooplankton are extirpated (Supplementary Fig.  
500 13). Reference #2 provides a detailed description of the model's original rationale and application.  
501 Here we show the reproducible Netlogo code (Supplementary Note 5) and the model parameters  
502 (Supplementary Table 7). To investigate the impact of the size of the ecosystem on the duration of  
503 the regime shift, we increased the carrying capacity of algae (K) by one, varying from 1 to 100 whilst  
504 maintaining constant parameters for all other variables (Supplementary Table 7). Using the  
505 'BehaviorSpace' tool within Netlogo<sup>47</sup>, every variation of this model was run for 10,000 time steps,  
506 resulting in 100 model runs. To investigate the impact of the system fluidity on the duration of the  
507 regime shift, we varied the fraction of volume exchanged between inside and outside (d;  
508 Supplementary Fig. 12) between 0 and 1 in increments of 0.01 (maintaining all other variables as  
509 constant; Supplementary Table 7). Every variation of this model was run for 10,000 time steps. This  
510 process resulted in 101 model runs. The SH model can be obtained from ref. 2.

511

#### 512 **Identifying regime shift durations of modelled time-series**

513 The completed model runs detailed above were exported as comma-separated values and read into  
514 the statistical software R<sup>43</sup> for analyses. The University of Southampton supercomputer 'Iridis 4' was  
515 used to process the model outputs. To demark the start of the regime shifts for the WSP model that

516 starts stable (Supplementary Fig. 6), we used the breakpoints function within the R-package  
517 'strucchange'<sup>48</sup>. The breakpoint function is based upon finding significant deviations from stability in  
518 classical regression models, whereby the regression coefficients shift from one stable regime to  
519 another<sup>48</sup>. We assume *a priori* that the number of statistically distinct time-series segments is equal  
520 to two: (1) pre-collapse state, (2) collapsed state, for the wolves, sheep and grass trends. Therefore,  
521 the breakpoint function searches for a single optimal breakpoint for each trend. Then for wolves and  
522 sheep, the end of the shift occurs once their respective abundances equal zero (Supplementary Fig.  
523 7a,b), whilst the termination of the grass shift occurs once grass completely covers the system  
524 (Supplementary Fig. 7c). As detailed above, the Chilika model uses the same breakpoint strategy as  
525 the WSP model, with the breakpoint function detecting the shift from the first stable regime, and  
526 the end of the shift denoted by the first time-step that the fish population is less than 1% of the  
527 original fish population. The breakpoint function is not required for the LC, GoL or SH model runs, as  
528 the models starts in an unstable state and so the start of the regime shift coincides with the first  
529 time step of the model. Therefore, in the LC model, the shift duration is equal to the number of  
530 time-steps (from start) until all the system nodes have the same language state (Supplementary Fig.  
531 8). In the GoL model, the shift duration is equal to the number of time-steps (from start) until the  
532 model reaches a stable state in which either all cells are dead, or a stable mixed state has been  
533 maintained for 100 steps (Supplementary Fig. 9). Likewise, in the SH model, the shift duration is  
534 equal to the number of time-steps (from start) until the first timestep when the concentration of  
535 zooplankton equals zero (Supplementary Fig. 13). To produce the regression models from the  
536 modelled data (Fig. 3), the model runs that did not undergo shifts (as explained in this section) were  
537 omitted from analysis (Supplementary Table 9). Then, the log-log linear models were formulated,  
538 relating shift time to the variable of interest (Table 1). Variations in the rates of grass regrowth were  
539 accounted for within the WSP generalised linear models, to assess the effect of the independent  
540 variable (Table 1) on shift duration for a given disturbance rate.

541

542

#### 543 **Data availability**

544 All data generated or analysed during this study are included in this published article (and its  
545 supplementary information files).

546

#### 547 **Code availability**

548 All model code is freely available from the following citation numbers in the reference list below: 2  
549 and 21-25. The complete Lake Chilika fishery model can be obtained from the corresponding author.  
550 The code amendments used to produce results presented in this paper are detailed in  
551 Supplementary Notes 3-5.

552 References

- 553 1. UN. *Transforming Our World: the 2030 Agenda for Sustainable Development*. (2015).
- 554 2. Scheffer, M. *Critical Transitions in Nature and Society*. (Princeton University Press, 2009).
- 555 3. Pauly, D., Watson, R. & Alder, J. Global trends in world fisheries: impacts on marine  
556 ecosystems and food security. *Philos. Trans. R. Soc. B Biol. Sci.* **360**, 5–12 (2005).
- 557 4. Biggs, R., Carpenter, S. R. & Brock, W. A. Turning back from the brink: Detecting an impending  
558 regime shift in time to avert it. *Proc. Natl. Acad. Sci.* (2009). doi:10.1073/pnas.0811729106
- 559 5. Mac Nally, R., Albano, C. & Fleishman, E. A scrutiny of the evidence for pressure-induced  
560 state shifts in estuarine and nearshore ecosystems. *Austral Ecol.* **39**, 898–906 (2014).
- 561 6. Scheffer, M., Carpenter, S., Foley, J. A., Folke, C. & Walker, B. Catastrophic shifts in  
562 ecosystems. *Nature* **413**, 591–596 (2001).
- 563 7. Biggs, R. O., Peterson, G. D. & Rocha, J. C. C. The Regime Shifts Database: a framework for  
564 analyzing regime shifts in social-ecological systems. *Ecol. Soc.* **23**, 9 (2018).
- 565 8. Groffman, P. M. *et al.* Ecological thresholds: The key to successful environmental management  
566 or an important concept with no practical application? *Ecosystems* **9**, 1–13 (2006).
- 567 9. Lenton, T. M. *et al.* Tipping elements in the Earth’s climate system. *Proc. Natl. Acad. Sci.* **105**,  
568 1786–1793 (2008).
- 569 10. Dearing, J. A., Braimoh, A. K., Reenberg, A., Turner, B. L. & van der Leeuw, S. Complex Land  
570 Systems: the Need for Long Time Perspectives to Assess their Future. *Ecol. Soc.* **15**, 19 (2010).
- 571 11. Folke, C. Resilience: The emergence of a perspective for social–ecological systems analyses.  
572 *Glob. Environ. Chang.* **16**, 253–267 (2006).
- 573 12. Renaud, F., Birkmann, J., Damm, M. & Gallopín, G. Understanding multiple thresholds of  
574 coupled social–ecological systems exposed to natural hazards as external shocks. *Nat.*  
575 *Hazards* **55**, 749–763 (2010).
- 576 13. Boettiger, C. & Hastings, A. From patterns to predictions. *Nature* **493**, 157 (2013).
- 577 14. Drijfhout, S. *et al.* Catalogue of abrupt shifts in Intergovernmental Panel on Climate Change  
578 climate models. *Proc. Natl. Acad. Sci.* **112**, E5777–E5786 (2015).
- 579 15. Olsson, P. *et al.* Shooting the Rapids: Navigating Transitions to Adaptive Governance of Social-  
580 Ecological Systems. *Ecol. Soc.* **11**, (2006).
- 581 16. Scheffer, M. *et al.* Anticipating Critical Transitions. *Science (80-. )*. **338**, 344–348 (2012).
- 582 17. West, G. *Scale: The Universal Laws of Life and Death in Organisms, Cities and Companies*.  
583 (Weidenfeld & Nicolson, 2017).
- 584 18. Hatton, I. A. *et al.* The predator-prey power law: Biomass scaling across terrestrial and  
585 aquatic biomes. *Science (80-. )*. **349**, aac6284 (2015).

- 586 19. Albert, R., Jeong, H. & Barabasi, A.-L. Error and attack tolerance of complex networks. *Nature*  
587 **406**, 378–382 (2000).
- 588 20. RA & SFI. Thresholds and alternate states in ecological and social-ecological systems.  
589 *Resilience Alliance and Sante Fe Institute* (2004).
- 590 21. Wilensky, U. NetLogo Wolf Sheep Predation Model. *Center for Connected Learning and*  
591 *Computer-Based Modeling, Northwestern University, Evanston, IL* (1997). Available at:  
592 <http://ccl.northwestern.edu/netlogo/models/WolfSheepPredation>. (Accessed: 25th June  
593 2016)
- 594 22. Wilensky, U. NetLogo Life model. *Center for Connected Learning and Computer-Based*  
595 *Modeling, Northwestern University, Evanston, IL* (1998). Available at:  
596 <http://ccl.northwestern.edu/netlogo/models/Life>. (Accessed: 25th June 2016)
- 597 23. Troutman, C. & Wilensky, U. NetLogo Language Change Model. *Center for Connected*  
598 *Learning and Computer-Based Modeling, Northwestern University, Evanston, IL* (2007).  
599 Available at: <http://ccl.northwestern.edu/netlogo/models/LanguageChange>. (Accessed: 20th  
600 June 2016)
- 601 24. Troutman, C., Clark, B. & Goldrick, M. Social networks and intraspeaker variation during  
602 periods of language change. *Univ. Pennsylvania Work. Pap. Linguist.* **14**, 16 (2008).
- 603 25. Cooper, G. S. & Dearing, J. A. Modelling future safe and just operating spaces in regional  
604 social-ecological systems. *Sci. Total Environ.* **651**, 2105–2117 (2019).
- 605 26. Bestelmeyer, B. T. *et al.* Analysis of abrupt transitions in ecological systems. *Ecosphere* **2**,  
606 art129 (2011).
- 607 27. Levine, N. M. *et al.* Ecosystem heterogeneity determines the ecological resilience of the  
608 Amazon to climate change. *Proc. Natl. Acad. Sci.* **113**, 793 LP – 797 (2016).
- 609 28. Brienen, R. J. W. *et al.* Long-term decline of the Amazon carbon sink. *Nature* **519**, 344 (2015).
- 610 29. de Bolle, M. *The Amazon Is a Carbon Bomb: How Can Brazil and the World Work Together to*  
611 *Avoid Setting It Off? PIIE: Policy Brief* **19–15**, (2019).
- 612 30. Lovejoy, T. E. & Nobre, C. Amazon Tipping Point. *Sci. Adv.* **4**, (2018).
- 613 31. Spalding, M. . & Grenfell, A. . New estimates of global and regional coral reef areas. *Coral*  
614 *Reefs* **16**, 225–230 (1997).
- 615 32. Gardner, T. A., Côté, I. M., Gill, J. A., Grant, A. & Watkinson, A. R. Long-Term Region-Wide  
616 Declines in Caribbean Corals. *Science (80- )*. **301**, 958 LP – 960 (2003).
- 617 33. Jackson, J. B. C., Donovan, M. K., Cramer, K. L. & Lam, W. *Status and Trends of Caribbean*  
618 *Coral Reefs: 1970-2012*. (2014).
- 619 34. Gray, L. A Mathematician Looks at Wolfram’s New Kind of Science. *Not. Am. Math. Soc.* **50**,

620 200–211 (2003).

621 35. Brose, U., Ostling, A., Harrison, K. & Martinez, N. D. Unified spatial scaling of species and their  
622 trophic interactions. *Nature* **428**, 167–171 (2004).

623 36. Tews, J. *et al.* Animal species diversity driven by habitat heterogeneity/diversity: the  
624 importance of keystone structures. *J. Biogeogr.* **31**, 79–92 (2004).

625 37. Rocha, J. C., Peterson, G., Bodin, Ö. & Levin, S. Cascading regime shifts within and across  
626 scales. *Science (80-. )*. **362**, 1379 LP – 1383 (2018).

627 38. Lewis, D. ‘Deathly silent’: Ecologist describes Australian wildfires’ devastating aftermath.  
628 *Nature* **577**, 304 (2020).

629 39. Cho, S. J. & McCarl, B. A. Climate change influences on crop mix shifts in the United States. *Sci.*  
630 *Rep.* **7**, 40845 (2017).

631 40. Steffen, W., Broadgate, W., Deutsch, L., Gaffney, O. & Ludwig, C. The trajectory of the  
632 Anthropocene: The Great Acceleration. *Anthr. Rev.* **2**, 81–98 (2015).

633 41. Steffen, W. *et al.* Trajectories of the Earth System in the Anthropocene. *Proc. Natl. Acad. Sci.*  
634 **115**, 8252 LP – 8259 (2018).

635 42. Scheffer, M. & van Nes, E. H. Seeing a global web of connected systems. *Science (80-. )*. **362**,  
636 1357 LP – 1357 (2018).

637 43. R. R: *A language and environment for statistical computing*. R Foundation for Statistical  
638 Computing. (2008).

639 44. Wilkinson, M. D. *et al.* The FAIR Guiding Principles for scientific data management and  
640 stewardship. *Sci. Data* **3**, 160018 (2016).

641 45. Wilensky, U. & Beisman, K. Connected Science: Learning Biology through Constructing and  
642 Testing Computational Theories – an Embodied Modeling Approach. *Int. J. Complex Syst.*  
643 **M.234**, 1–12 (1999).

644 46. Wilensky, U. & Beisman, K. Thinking Like a Wolf, a Sheep, or a Firefly: Learning Biology  
645 Through Constructing and Testing Computational Theories—An Embodied Modeling  
646 Approach. *Cogn. Instr.* **24**, 171–209 (2006).

647 47. Wilensky, U. NetLogo. (1999). Available at: <http://ccl.northwestern.edu/netlogo/>. (Accessed:  
648 20th June 2017)

649 48. Zeileis, A. *et al.* Package ‘strucchange’. 69 (2015). Available at: [https://cran.r-](https://cran.r-project.org/web/packages/strucchange/strucchange.pdf)  
650 [project.org/web/packages/strucchange/strucchange.pdf](https://cran.r-project.org/web/packages/strucchange/strucchange.pdf). (Accessed: 11th February 2016)

651

652 **Acknowledgements**

653 GSC and JAD gratefully acknowledge a research studentship and financial support respectively from  
654 the Deltas, Vulnerability and Climate Change: Migration and Adaptation (DECCMA) project under  
655 the Collaborative Adaptation Research Initiative in Africa and Asia (CARIAA) program with financial  
656 support from the UK Government's Department for International Development (DFID) and the  
657 International Development Research Centre (IDRC), Canada (Grant No. 107642-001). The views  
658 expressed in this work are those of the creators and do not necessarily represent those of DFID and  
659 IDRC or its Boards of Governors. SW was funded by UKRI project numbers: NE/L001322/1,  
660 NE/T00391X/1, ES/R009279/1 and ES/R006865/1. We thank Professor Peter Langdon (University of  
661 Southampton) for providing early contributions to the concepts of this paper and Dr Rong Wang  
662 (Nanjing Institute of Geography and Limnology) for preliminary data collection and analysis. We also  
663 thank Dr James Dyke (University of Southampton), Professor Felix Eigenbrod (University of  
664 Southampton) and Dr Robert Cooke (University of Southampton) for their comments on earlier  
665 versions of the manuscript. We also wish to acknowledge the use of the IRIDIS High Performance  
666 Computing Facility, and associated support services at the University of Southampton, in the  
667 completion of this work.

668

669 **Author contributions**

670 GSC contributed towards the 'empirical data collection', 'analysis of model outputs' and 'manuscript  
671 writing'. SW contributed towards the 'study design', 'computational modelling', 'analysis of model  
672 outputs' and 'manuscript writing'. JAD contributed towards the 'study design', 'theoretical  
673 development' and 'manuscript writing'

674

675 **Competing interests**

676 The authors declare no competing interests.

677

678 **Figure legends and tables**

679 **Figure 1|** Graphical representation of the modelling framework. Each row shows two graphics to  
680 illustrate the extreme variants (low, high) for a specific metric associated with either system size  
681 (upper) or fluidity (lower) in the twelve modelling experiments.

682

683 **Figure 2|** Empirical relationship between system area and regime shift duration. A) The log-log  
 684 linear relationship between the spatial area and the temporal duration of 42 observed Earth system  
 685 regime shifts is described by a linear regression model (solid line:  $R^2 = 0.491$ ,  $p < 0.001$ ,  $df = 40$ ). This  
 686 illustrates the positive and sub-linear (slope = 0.221) association between system size and shift  
 687 duration. B) The relationship in A is compared to the 1:1 reference line (dashed line, slope = 1). The  
 688 untransformed unit of the x-axis is kilometres-squared, whilst the y-axis is years. The shading  
 689 represents the 95% confidence interval around the regression model; see Supplementary Table 1 for  
 690 individual case study details and see Supplementary Fig. 4 for the regression models grouped by  
 691 system type.

692

693 **Figure 3|** Modelled outputs exploring the relationships between regime shift duration and twelve  
 694 spatial characteristics. The trend lines and regression coefficients resulting from the twelve  
 695 simulation experiments (#1.1-#5.2) show the effects of different spatial properties on the duration  
 696 of system shift (Table 1). Dashed lines are 1:1 reference lines plotted with a y-intercept of '0'. Log-  
 697 log axes are used for consistency with Fig. 1, with the 'b-term' representing the slope of the  
 698 regression model. See Supplementary Table 8 for the linear model coefficients and comparisons.

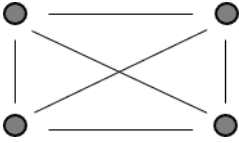
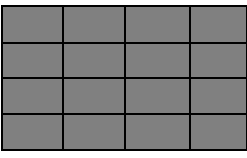
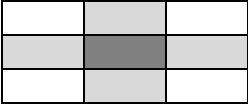
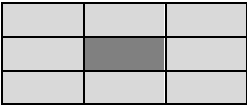
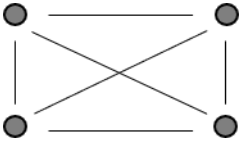
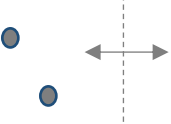
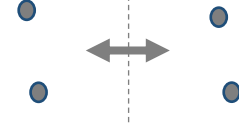
699

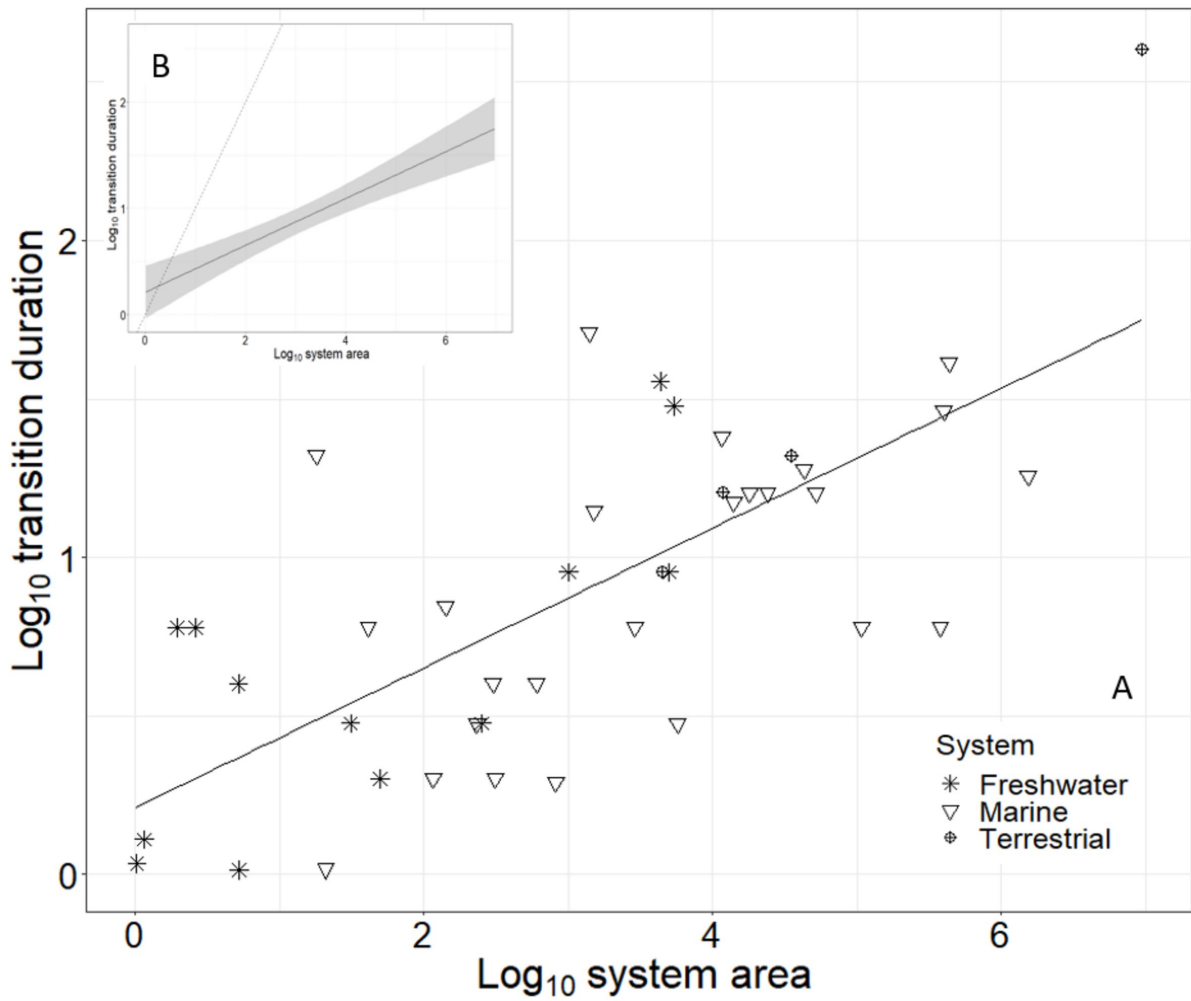
Table 1 | Details and hypotheses of the twelve modelling experiments designed to substantiate the empirical relationship observed in Fig. 1. See Methods and Supplementary Notes 3-5 for additional and replicable details on the structure, parameterisation and code of the models.

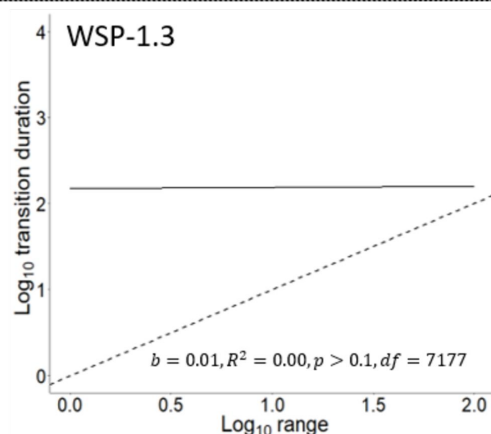
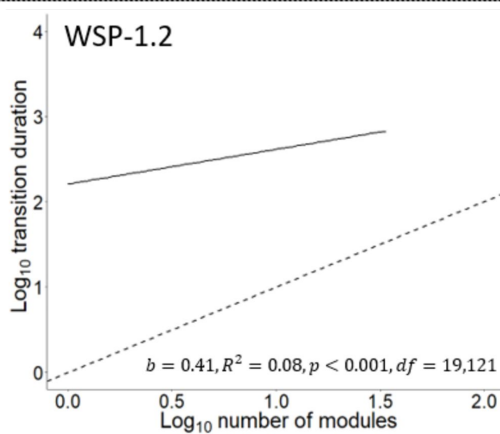
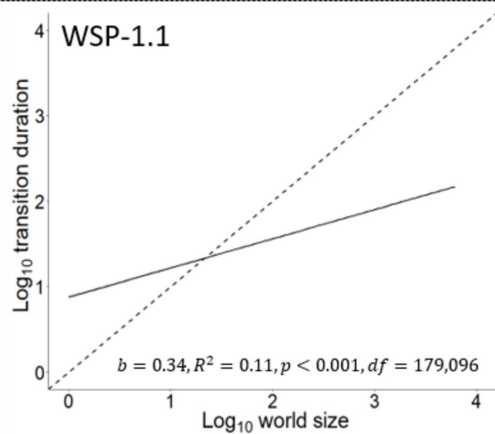
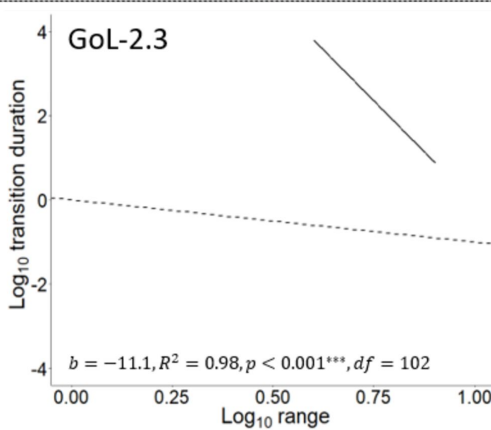
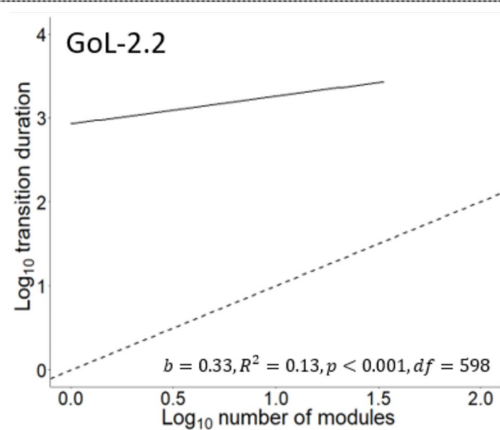
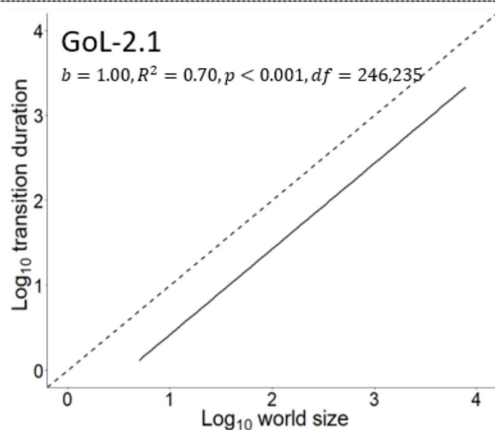
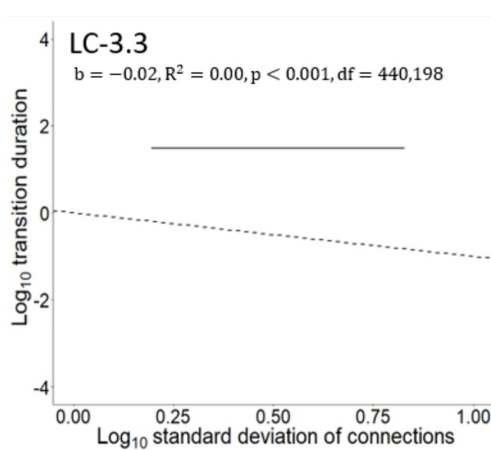
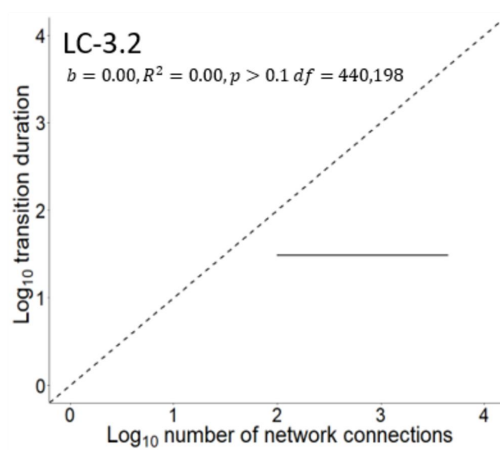
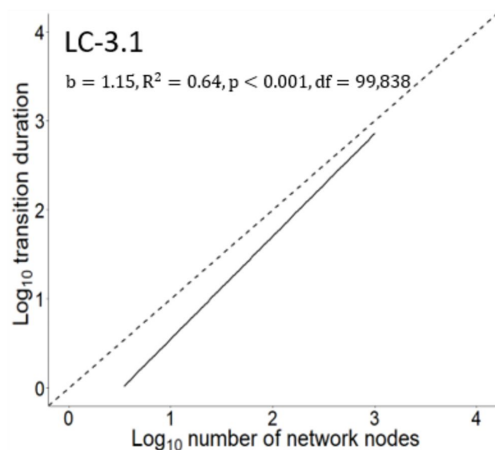
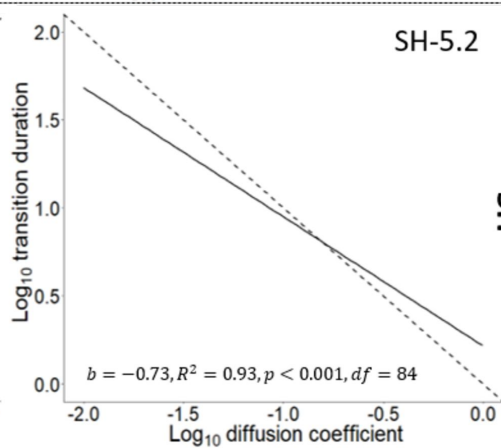
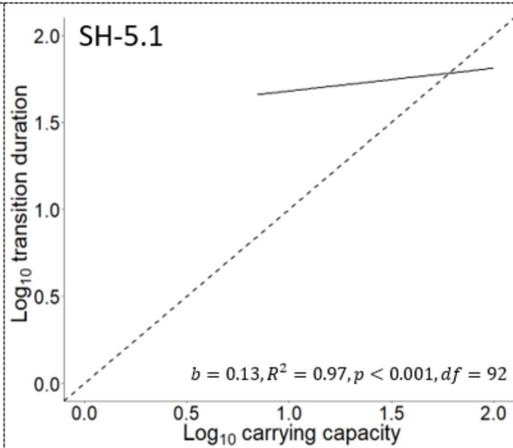
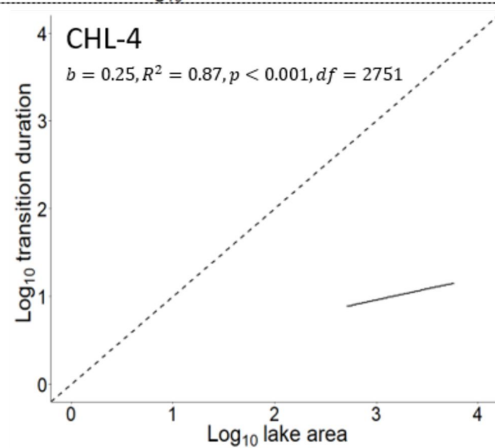
Model name	Model type	Parameter varied (experiment num.)	Parameter range	Repeats per parameter value	NumberHypothesis of runs (n)
Wolf-Sheep Predation (WSP)	Agent-based	1.1. Model total area	World height: [0-100] World width: [0-100].	100	260,100 Larger system areas should exhibit longer shift durations
		(1.2) Module size (divide constant 100 x 100 area into 100) <sup>†</sup> sub-worlds)	[2, 5, 10, 20, 50,	100	60,600 More modular systems should exhibit longer shift durations

		(1.3) Maximum distance wolves and sheep can move per timestep	[1-100 cells]	100	10,000	More fluid systems should exhibit shorter shift durations
Game of Life (GoL)	Cellular automata	(2.1) Model total area	World height: [0-100] World width: [0-100].	100	260,100	Larger system areas should exhibit longer shift durations
		(2.2) Module size (divide constant 100 x 100 area into discrete sub-worlds)	[2, 5, 10, 20, 50, 100]	100	600	More modular systems should exhibit longer shift durations
		(2.3) Number of neighbouring cells any one cell can interact with	4 or 8	100	200	More fluid systems should exhibit shorter shift durations
Language Change (LC)	Network-structured	(3.1) Number of network nodes	[3 – 1000]	100	99,800	Networks with more nodes should exhibit longer shifts
		(3.2) Number of inter-nodal connections	[99 – 4,500]	100	440,200	Networks with more connections should exhibit longer shifts
		(3.3) Standard deviation of connections measured from experiment 3.2.	[99 – 4,500]	100	440,200	Networks with more homogenous connections should exhibit longer shifts
Lake Chilika (CHL)	System dynamics model	(4) Model total area	[500-10,000 km <sup>2</sup> ]	5000 areas randomly sampled between limits	5000	Larger system areas should exhibit longer shift durations
Spatial Heterogeneity (SH)	Ordinary differential equation	(5.1) Carrying capacity for phytoplankton (i.e. model size)	[1-100]	1 (model does not have stochasticity)	101	Large systems should exhibit longer shift durations
		(5.2) Fraction of volume exchanged between model parts (i.e. diffusion of stress)	[1-100]	1 (model does not have stochasticity)	101	More fluid systems should exhibit shorter shift durations

<sup>†</sup>The grass regrowth rate in experiment WSP-1.2 was also varied 1-100 and statistically controlled for in our regression models (see Methods).

System component	Model metric	Low	High	Experiment
System size	Area			1.1, 2.1, 4
	Number of individuals			3.1, 5.1
	Number of connections			3.3
Fluidity	Number of modules			1.2, 2.2
	Movement ability			1.3
	Interaction distance	 Dark interacts with light	 Dark interacts with light	2.3
	Evenness of connections			3.2
	Fraction exchanged			5.2



**WSP****GOL****LC****CHL****HS**